

## **The application of advanced TEM techniques to the characterisation of an asymmetric spacer layer tunnel diode**

**D Cooper, A C Twitchett, R E Dunin-Borkowski, D Zhi, M J Kelly<sup>1</sup> and P A Midgley**

Department of Materials Science and Metallurgy, University of Cambridge, Pembroke Street, Cambridge, CB2 3QZ

<sup>1</sup> Department of Engineering, University of Cambridge, Trumpington Street, Cambridge, CB2 1PZ

**ABSTRACT:** The advent of commercially available field emission TEMs has seen the emergence of new techniques for high spatial resolution analysis of interfaces and boundaries. Electron holography is one such technique and in this paper we have examined an asymmetric spacer layer tunnel diode using two forms of electron holography to elucidate the structure and composition of a thin AlAs quantum well buried within a GaAs substrate. The sensitivity of the holographic methods shows how such wells can be examined with high accuracy.

### **1. INTRODUCTION**

Unlike more conventional microwave detectors, such as the Schottky diode or planar-doped-barrier diode, the asymmetric spacer layer tunnel (ASPAT) diode manages to combine a range of desired properties that include wide dynamic range, low excess noise and low sensitivity to ambient temperature (Kelly 2002). However, a major problem with manufacturing the ASPAT diode is the reproducibility of the barrier thickness. A small change in the thickness of this barrier has important consequences for the forward bias characteristics of the diode. It is therefore essential to characterise the width of this barrier accurately and reproducibly. The scale of the barrier is such that high spatial resolution electron microscopy is the only tool capable of yielding the necessary information. In particular, it is the electronic characteristics of the structure that are key to the device performance and thus, ideally, any microscopy undertaken should be sensitive to the electrostatic potential and not simply to the structure of the device.

Electron holography provides the ability to record not only the amplitude of a scattered wave but also its phase. The phase difference between regions of different doping or composition produce modulations in the interference fringes of an off-axis hologram. Fourier analysis is used to extract this phase information in a quantitative and precise way. In this paper, we have used two forms of electron holography. The first is off-axis electron holography, Fig. 1, in which an electron biprism is used to split a coherent wavefront, allowing interference fringes to be recorded on a charge coupled detector (CCD) camera. Reconstructing the phase is then relatively straightforward using well-established techniques (Midgley 2001). The second method is in-line electron holography, also known as Fresnel imaging, in which a series of images are taken at successive defocus settings. Direct recovery of the phase is then not straightforward. Iterative routines, such as the Gerchburg-Saxton algorithm, can be applied but these can lead to artefacts and may not converge to a global minimum. More usually, a multi-parameter model based on sensible physical parameters is varied in a systematic fashion in order to achieve a best fit. This has been our approach in this paper.

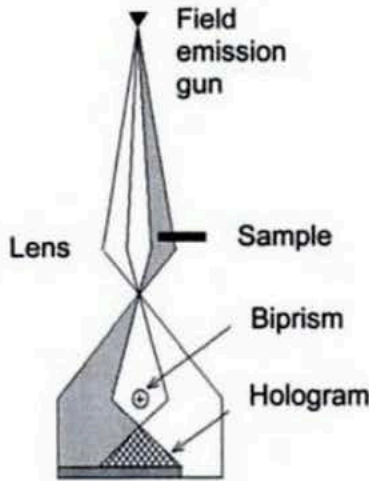


Fig. 1. Schematic diagram of the formation of an off-axis electron hologram.

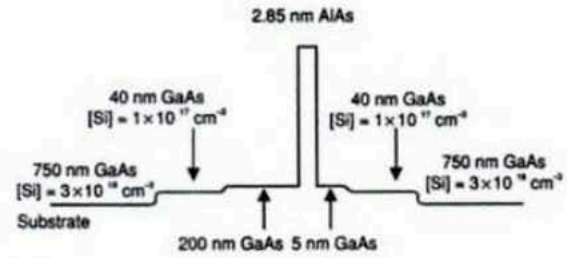


Fig. 2. A schematic diagram of the structure of the ASPAT diode studied in this paper. After Kelly (2002).

## 2. SAMPLE PREPARATION AND CONVENTIONAL IMAGING

The ASPAT diode, whose nominal structure is shown in Fig. 2, was prepared in cross-section using an FEI 200 focused ion beam (FIB) workstation. FIB milling was chosen over more conventional sample preparation techniques because it provides a sample with a relatively large flat area of uniform thickness and allows cuts to be made perpendicular to the surface so that the buried structure can be 'accessed' from the side of the device. This capability is important for off-axis electron holography as part of the electron wavefront should pass through a region of space with a uniform reference phase (in this case vacuum). The sample was stored carefully under dry vacuum to ensure minimal damage to the AlAs layer, which is prone to oxidation in air.



Fig. 3. 200 dark field image showing the Al-rich quantum well.

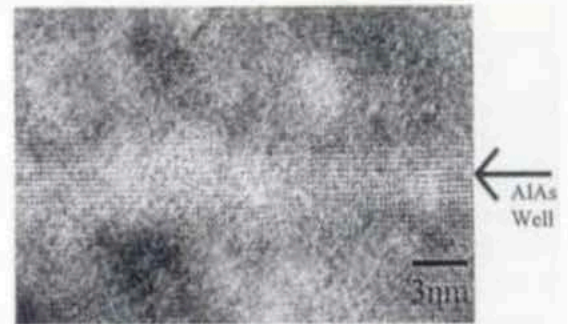


Fig. 4. High-resolution image revealing the Al-rich well (marked).

Figure 3 shows a 200 dark field image in which the Al-rich quantum well is revealed. The 200 reflection is known to be sensitive to the change in the composition of the group III metal in III-V systems. In the kinematic limit, the image intensity is proportional to the atomic number difference. Thus, AlAs appears brighter than GaAs. The slight waviness indicates an apparent modulation in the thickness of the barrier. A more accurate measurement of the barrier width can be made using high resolution electron microscopy. A lattice image is shown in Fig. 4, in which the 200 and 220 spots were included in the objective aperture. Interpretation is not straightforward, but the image still shows chemical contrast and the apparent barrier width can be measured to within approximately a monolayer. An average width of  $3.40 \pm 0.43$  nm is found, somewhat larger than expected.



### 3. IN-LINE ELECTRON HOLOGRAPHY (FRESNEL IMAGING)

In-line electron holography (Fresnel imaging) is remarkably sensitive to changes in the mean inner potential of an interface and thus to changes in atomic number density, (Ross and Stobbs 1991). A series of energy filtered bright-field images of the AlAs barrier layer was acquired at different defoci using the Philips CM300 FEGTEM. After correcting for magnification changes and rotation, and having carefully calibrated the defocus steps using power spectra of carbon foils, a series of line scans across the barrier were compared with simulations of varying parameters that described the layer using a simplex algorithm.

Figure 5(a) shows a montage of line traces extracted from a region of the barrier at different defoci. The sample thickness was determined using convergent beam electron diffraction (CBED) to be 135nm and was one of the fixed input parameters to the model used to produce a best fit to the data which is shown in Fig.5(b). In order to compare the fit in more detail, Fig. 5(c) shows the experimental and calculated intensities at the defocus settings indicated. The agreement is excellent. Fig. 5(d) shows the best-fitting complex potential. It is a Gaussian well, whose real part has a full width half maximum (FWHM) of 3.63nm and a depth of 0.81V. The imaginary part was 19% of the real part and remained negative, indicating that the Al-rich layers scattered the electron beam less strongly than the surrounding GaAs.

The potential difference between the AlAs well and the GaAs was determined to be 0.81V, lower than would be expected from a simple neutral atom scattering factor calculation. This could be for three reasons. Firstly, the mean inner potentials of the two materials will be altered by the effects of bonding (Kruse 2002). Secondly, despite keeping the sample in a controlled environment the layer may have oxidised, leading to perhaps some grooving and a reduction in thickness of the layer; this would lead to an apparent reduction in potential. Thirdly, the images may contain a contribution from diffuse (e.g. phonon) scattering, even though they are energy filtered.

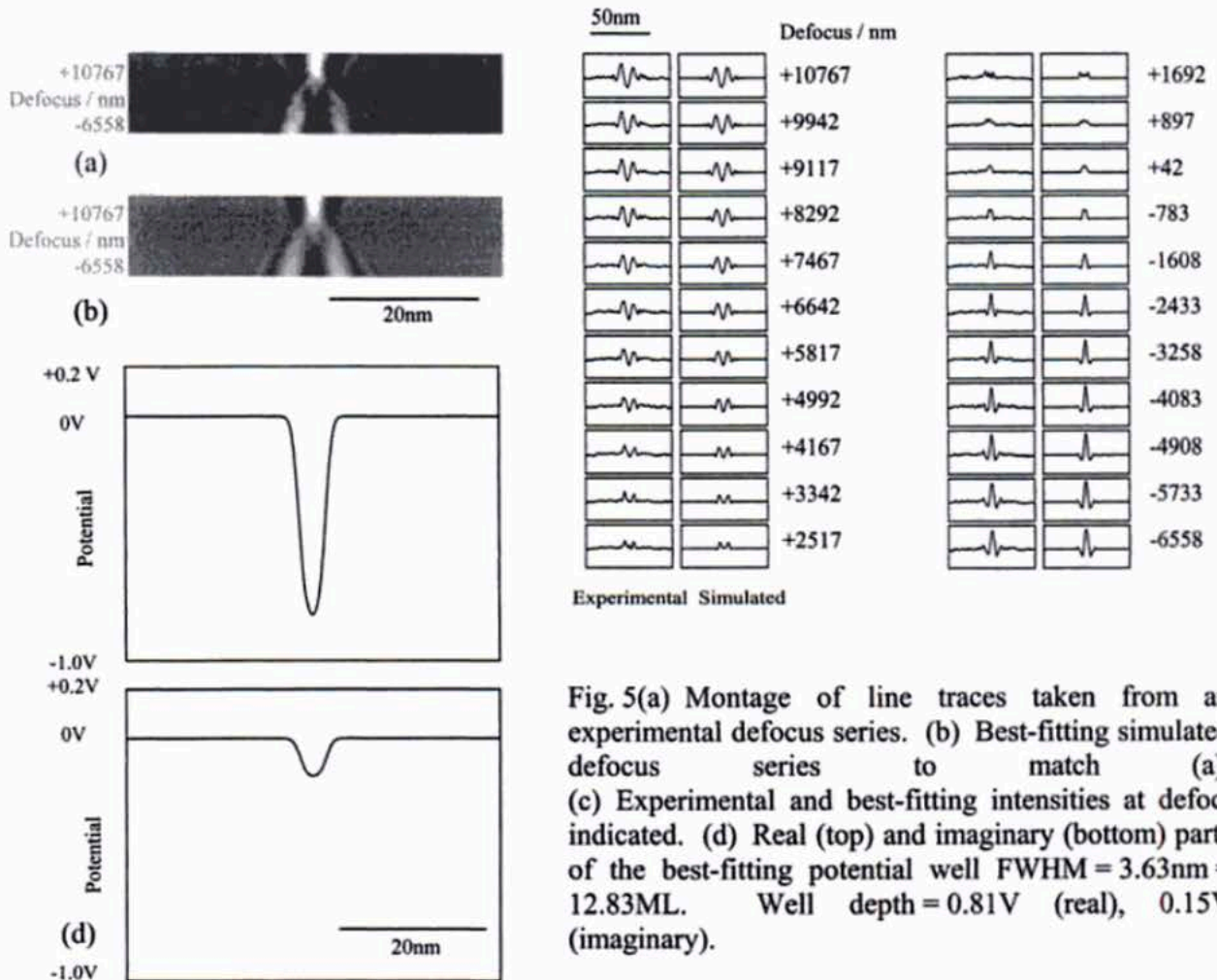


Fig. 5(a) Montage of line traces taken from an experimental defocus series. (b) Best-fitting simulated defocus series to match (a). (c) Experimental and best-fitting intensities at defoci indicated. (d) Real (top) and imaginary (bottom) parts of the best-fitting potential well FWHM = 3.63nm = 12.83ML. Well depth = 0.81V (real), 0.15V (imaginary).



#### 4. OFF-AXIS ELECTRON HOLOGRAPHY

Using the Philips CM300 FEGTEM off-axis electron holograms of the AlAs barrier were recorded at high magnification with the main objective lens of the microscope turned on. The holograms were processed to yield amplitude and phase images of the ASPAT diode structure. Assuming weak diffraction, the unwrapped phase (removing any  $2\pi$  phase jumps) is proportional to the product of the mean inner potential,  $V_0$ , and the projected thickness of the sample. If the thickness is measured independently, in our case using convergent beam electron diffraction, then the change in the mean inner potential can be measured across the layer. Knowing the mean inner potential for pure GaAs and pure AlAs, a measure of the composition can then be obtained.

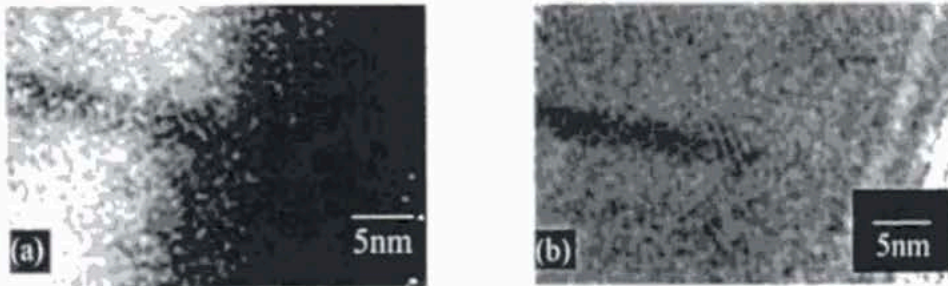


Fig. 6. Reconstructed (a) phase and (b) amplitude images showing the AlAs barrier.

Figure 6 shows (a) the reconstructed phase and (b) the amplitude image for a region near the AlAs barrier in the ASPAT diode. The reconstructed images are noisy and the contrast weak but nevertheless the layer is evident. From the reconstructed phase it is possible to measure the potential depth and width as before. Using this technique, we find the potential well to be only 0.6V in depth with a FWHM of  $3.8 \pm 0.4$ nm. The discrepancy between the well depths measured using the two techniques may result from noise in the off-axis data or be due to the fact that a damaged region close to the sample edge was examined.

#### 5. CONCLUSIONS

In line holography (Fresnel imaging) and off axis holography have been used to calculate the width and depth of the potential barrier associated with an AlAs quantum well in an ASPAT diode.

Both techniques gave similar barrier widths, larger than expected and well depths lower than predicted by calculation. The apparent increase in width may again be brought about by the degradation of the layer. Any grooving will tend to affect off-axis holography more than Fresnel imaging as it is more sensitive to the low frequency changes in thickness and potential.

#### ACKNOWLEDGEMENTS

We would like to thank the EPSRC, Newnham College and the Royal Society for their financial support.

#### REFERENCES

- Kelly M J 2002 Electronics and Communications Journal April 73
- Kruse P, Rosenauer A and Gerthsen D 2002 Ultramicroscopy **96** 11
- Midgley P A 2001 Micron **32** 167
- Ross F and Stobbs M 1991 Ultramicroscopy **36** 331